



Roles of Spin-dependent Transitions in Nuclei on Astrophysical Processes in Stars

Toshio SUZUKI¹, Michio HONMA², Noritaka SHIMIZU³, Takaharu OTSUKA^{4,5}, Kanji MORI⁶ and Toshitaka KAJINO⁷

¹*Department of Physics, College of Humanities and Sciences, Nihon University, 3-25-40 Sakurajosui, Setagaya, Tokyo 156-8550, Japan*

²*Center for Mathematical Sciences, University of Aizu, Aizu-Wakamatsu, Fukushima 965-8580, Japan*

³*Center for Nuclear Study, The University of Tokyo, 7-3-1 Hongo, Bunkyo, Tokyo 113-0033, Japan*

⁴*Department of Physics, The University of Tokyo, 7-3-1 Hongo, Bunkyo, Tokyo 113-0033, Japan*

⁵*RIKEN Nishina Center, 2-1 Hirosawa, Wako, Saitama 351-0198, Japan*

⁶*Research Institute of Stellar Explosive Phenomena, Fukuoka University, 8-19-1 Nanakuma, Jonan-ku, Fukuoka-shi, Fukuoka 814-0180, Japan*

⁷*School of Physics, Beihang University, Haidian-qu, Beijing 100083, People's Republic of China*

E-mail: suzuki@chs.nihon-u.ac.jp

(Received January 11, 2022)

Electron-capture and β -decay rates in stellar environments are evaluated by shell-model calculations with new shell-model Hamiltonians which can describe Gamow-Teller (GT) transitions in nuclei quite well. The weak rates in *sd*-shell nuclei are used to study nuclear Urca processes in ONeMg cores of $8\text{-}10M_{\odot}$ stars. The GT transitions and weak rates of nuclear pairs with $A=31$ in *sd-pf* shell and $A=61$ in *pf*-shell relevant to Urca processes in neutron star crusts are evaluated and discussed. The weak rates in *pf*-shell are applied to study nucleosynthesis of iron-group elements in Type Ia supernova explosions.

KEYWORDS: Gamow-Teller transition, e-capture, β -decay, Urca process, nucleosynthesis ...

1. Introduction

Weak transition rates in stellar environments relevant to astrophysical processes in stars are evaluated with new shell-model Hamiltonians in *sd*-shell, *pf*-shell and *sd-pf* shell, which can describe spin responses in nuclei quite well. Electron-capture and β -decay rates thus obtained are applied to study nuclear Urca processes in stars and nucleosynthesis in supernova (SN) explosions. As the dominant contributions to the weak rates come from GT transitions, new shell-model calculations lead to remarkable improvements in the weak rates. In Sect. 2, we discuss the weak rates in $A=23$ and 25 nuclear pairs and Urca processes in ONeMg cores in $8\text{-}10M_{\odot}$ stars, as well as the rates in $A=31$ and 61 nuclear pairs relevant to Urca processes in neutron star crusts. In Sect. 3, synthesis of neutron-rich iron group nuclides in Type Ia supernovae is discussed with the weak rates updated in *pf* shell.

2. Electron-capture and β -decay rates and nuclear Urca processes

Electron-capture and β -decay rates in *sd* shell obtained by USDB Hamiltonian [1] in stellar environments, that is, at high temperatures ($T = 10^8\text{-}10^{10}$ K) and high densities ($\rho Y_e = 10^8\text{-}10^{10}$ g cm $^{-3}$ with Y_e the electron fraction) are applied to nuclear Urca processes. The e-capture rates increase while the β -decay rates decrease as the density increases due to the increase of electron chemical



potential at high densities. Both the weak rates coincide at a certain density, called a Urca density, almost independent of temperatures. Both ν and $\bar{\nu}$ are emitted at the Urca density thus taking away the energy from the star, which results in a drastic cooling of the core of the star. This mechanism, called the nuclear Urca process, occurs quite efficiently for the nuclear pairs with $A = 23$ and 25 , where the transitions between the ground states are GT ones [2, 3]. Urca densities for the nuclear pairs, ^{25}Mg - ^{25}Na and ^{23}Na - ^{23}Ne , are $\log_{10}(\rho Y_e) = 8.78$ and 8.92 , respectively. The weak rates for the nuclear pair, ^{25}Mg - ^{25}Na , and the cooling of ONeMg core of a star with $8.8 M_\odot$ are shown in Fig. 1 [2, 4]. When Coulomb corrections from electron background, that is, the screening (SCR) effects are included, ion-electron potential and chemical potential of ions are modified [5, 6]. The latter changes the threshold energy of a reaction, which results in a reduction of e-capture rate and an enhancement of β -decay rate. The SCR shifts the Urca density to a higher density region by $\Delta \log_{10}(\rho Y_e) = 0.03$ [2, 3].

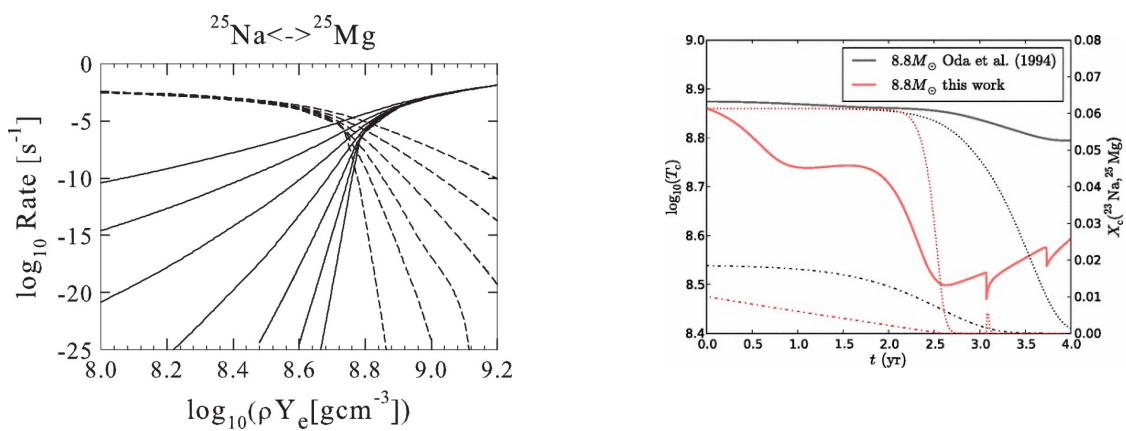


Fig. 1. (Left) Weak rates for the $A=25$ Urca nuclear pair, ^{25}Mg - ^{25}Na , as functions of density $\log_{10}\rho Y_e$ at temperatures in the range of $\log_{10}T = 8$ to 9.2 in steps of 0.2 . Electron-capture and β -decay rates are denoted by solid and dashed lines, respectively. Taken from [3]. (Right) The evolution of the central temperature T_c of an ONeMg core of the $8.8 M_\odot$ star as a function of time in units of years. The temperature drop up to $t=1$ year and the temperature drop during $t= 2-2.5$ year are caused by the Urca processes by the $A=23$ and $A=25$ nuclear pairs, respectively. Changes of the mass fraction X_c of ^{25}Mg and ^{23}Na are also shown. The case with the use of Oda et al.'s table [7] using sparse grid is also shown, where there is no effect of the Urca process. Taken from [2].

The star with $8.8 M_\odot$ collapses triggered by subsequent e-capture processes on ^{24}Mg and ^{20}Ne , and ends with an e-capture (EC) SN explosion. Stars with $M > 9 M_\odot$ are likely to end with core-collapse (CC) SN explosions. Border of CC-SN or EC-SN is at $M \sim 9 M_\odot$, and the fate of the stars with $8-10 M_\odot$ is sensitive to nuclear weak rates as well as their masses.

Next, we discuss a nuclear Urca process for a nuclear pair in the island of inversion [8]. Several nuclear pairs have been pointed out to be important for the cooling of neutron star crusts [9]. Here, the pair with $A = 31$ in the island of inversion, $^{31}\text{Mg} \leftrightarrow ^{31}\text{Al}$, is considered as it is one of the potential candidates that contribute to the cooling [9, 10].

Neutron-rich nuclei in the island of inversion (sd - pf shell) are studied by shell-model calculations with the EEdf1 interaction [12] obtained by the extended Kuo-Krenciglowa (EKK) method [11] starting from chiral EFT $N^3\text{LO}$ and Fujita-Miyazawa 3N interaction [13]. Neutron ESP's between sd -shell and pf -shell orbits become much closer in the n-rich region, $Z = 10-12$, for the EEdf1 compared with conventional sd - pf shell Hamiltonians such as sd-pf-m [15]. This results in larger admixtures of

pf -shell components for the EEdf1: the contributions from 4p-4h excitations are found to be larger than those from 2p-2h excitations in ^{32}Mg .

Energy levels of ^{31}Mg can be well explained by the EEdf1 [13]. Configurations including up to 6p-6h excitations are taken. The ground state (g.s.) of ^{31}Mg is calculated to be $1/2^+$ consistent with the experimental observation [16], while it is predicted to be $7/2^-$ by the sdpf-m. The first excited state is predicted to be $3/2^+$, very close to the ground state $1/2^+$. As the g.s. of ^{31}Al is $5/2^+$, GT transition between $3/2^+$ state in ^{31}Mg and $5/2_{g.s.}^+$ in ^{31}Al gives the main contribution to the e-capture and β -decay rates for the $A=31$ pair.

The weak rates in stellar environments obtained with the EEdf1 are shown in Fig. 2. The GT transitions between ^{31}Mg ($3/2^+, 1/2^+$) and ^{31}Al ($5/2^+, 1/2^+, 3/2^+$) are taken into account. Calculated $\log ft$ values are 5.43 and 7.40 for ^{31}Mg ($3/2^+$) \rightarrow ^{31}Al ($5/2^+$) and ($3/2^+$), respectively. Those for ^{31}Mg ($1/2^+$) \rightarrow ^{31}Al ($3/2^+$) and ($1/2^+$) are 5.98 and 5.78, respectively, while the experimental values are 5.59 and 6.025, respectively. Deviations of the calculated GT strengths from the experimental ones are rather moderate, by a factor of 0.4-1.8.

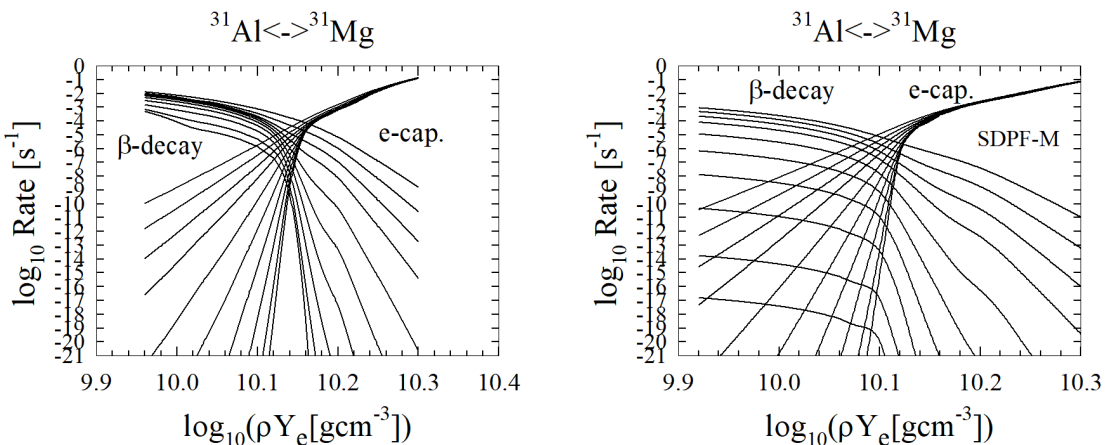


Fig. 2. Electron-capture and β -decay rates for the nuclear pair, ^{31}Al - ^{31}Mg , as functions of density $\log_{10}(\rho Y_e)$ for various temperatures. (Left) The rates are evaluated with the EEdf1 interaction obtained by the EKK method [13]. (Right) The rates are obtained with the sdpf-m Hamiltonian [15].

There exists a Urca density as shown in Fig. 2 (left panel) since the excitation energy of the $3/2^+$ state in ^{31}Mg is as small as 0.05 MeV. If the g.s. of ^{31}Mg is taken to be $7/2^-$, there does not exist a Urca Density as shown in Fig. 2 (right panel) because of non-existence of GT transitions between low-lying states.

We finally discuss $A=61$ nuclear pair, $^{61}\text{Cr} \leftrightarrow ^{61}\text{V}$. A QRPA calculation predicts a rather strong GT transition strength for the β -decay $^{61}\text{V} \rightarrow ^{61}\text{Cr}$. If the g.s. to g.s. transition is assumed to be a GT one, the $A=61$ Urca pair is expected to give a large contribution to the cooling of the neutron star crusts. However, a recent β -decay experiment shows that the $\log ft$ value for the transition $^{61}\text{V}_{g.s.} \rightarrow ^{61}\text{Cr}_{g.s.}$ is $\log ft = 5.5 \pm 0.2$. This suggests a weaker transition strength compared with a value $\log ft = 4.35$ predicted by the QRPA. The GT strength for ^{61}V ($3/2^-, \text{g.s.}$) \rightarrow ^{61}Cr obtained by shell-model calculation with a pf -shell Hamiltonian GXPF1J [17] is shown in Fig. 3. A quenching factor of 0.74 is taken for g_A^{eff}/g_A . Calculated $\log ft$ value for the transition to the g.s. of ^{61}Cr ($5/2^-$) is $\log ft = 5.68$, consistent with the experimental value. Though spins of the g.s.'s were not assigned definitely by the experiment, the present shell-model calculation suggests $J^\pi = 3/2^-$ and $5/2^-$ for the g.s. of ^{61}V and ^{61}Cr , respectively. The e-capture and β -decay rates for the transitions between the g.s.

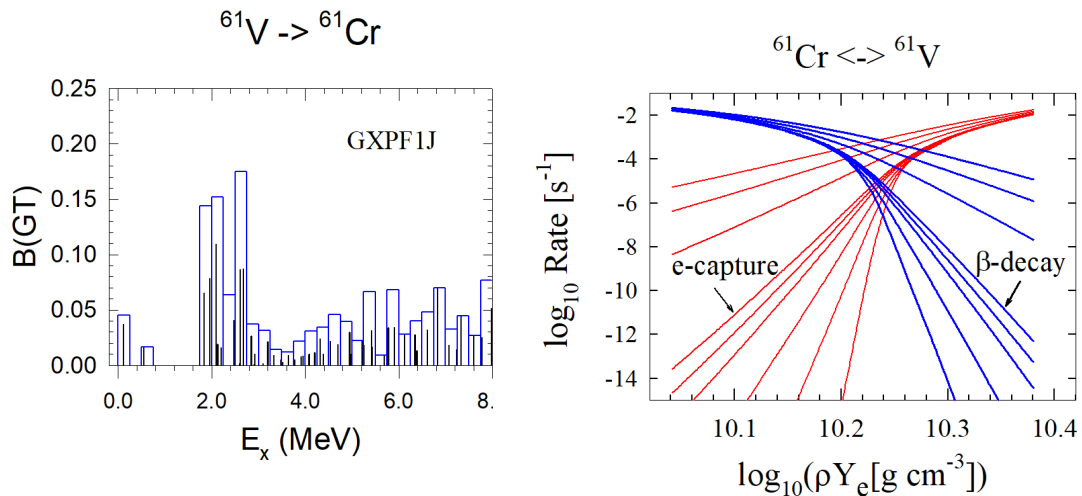


Fig. 3. (Left) GT strength for $^{61}\text{V} \rightarrow ^{61}\text{Cr}$ obtained with GXPF1J. (Right) Electron-capture and β -decay rates for the nuclear pair, $^{61}\text{Cr}-^{61}\text{V}$, as functions of density $\log_{10}(\rho Y_e)$ for various temperatures.

states obtained with the GXPF1J are shown in Fig. 3. There exists a Urca density around $\log_{10}(\rho Y_e) = 10.23$. A moderate contribution to the cooling from the $A=61$ nuclear pair is expected. Studies with extended shell-model configuration spaces with $g_{9/2}d_{5/2}$ shell are left to future.

3. Electron-capture rates in *pf* shell and synthesis of iron-group elements

GT strengths in Ni and Fe isotopes are described quite well with a new shell-model Hamiltonian, GXPF1J [17], in *pf* shell with a universal quenching factor $f = g_A^{eff}/g_A = 0.74$. In particular, the GT strength in ^{56}Ni obtained by (p, n) reaction has two-peak structure [18], and it can be reproduced well by the GXPF1J [19]. Calculated GT strength with the GXPF1J as well as those with KB3G [20] and KBF [21] and the experimental values are shown in Fig. 4. Both KB3G [20] and KBF [21] fail to reproduce the two-peak structure. The GXPF1J is shown to reproduce experimental e-capture rates in various *pf*-shell nuclei better than KB3G and RPA calculations [22].

The GT strength spreads more for GXPF1J compared with KB3G, which leads to smaller e-capture rates for GXPF1J. As the KBF, conventionally used for stellar calculations, take into account experimental data of energies and GT strength available, the e-capture rates of KBF come close to those of GXPF1J.

Now, we discuss synthesis of iron-group elements in Type Ia SN. Here, single-degenerate 'Chandra' model is treated. Accretion of matter from non-degenerate companion to a white dwarf (WD) occurs, and a SN explosion takes place when WD mass approaches the Chandrasekhar limit. A lot of ^{56}Ni is produced during the explosion, and successive e-capture reactions produce neutron-rich (n-rich) nuclides and Y_e decreases. Decrease of e-capture rates leads to less production of n-rich nuclides and larger Y_e .

There was an over-production problem of n-rich iron-group elements compared with the solar abundances when e-capture rates of FFN [24] were used. N-rich nuclei such as ^{54}Cr and ^{58}Ni are produced several times more than the solar abundances when an explosion model W7 with fast deflagration with subsonic frame front was used [25]. Another explosion model WDD2 [25] with slow deflagration and delayed detonation with supersonic shock wave is used also here. The production

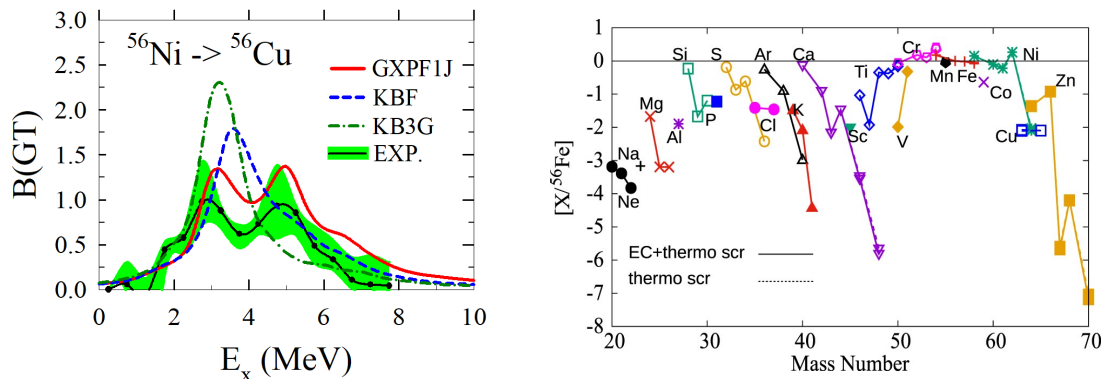


Fig. 4. (Left) The $B(GT)$ strengths obtained by shell-model calculations with GXPF1J (solid), KBF (dashed) and KB3G (dash-dotted) Hamiltonians. Experimental data [18] are also shown. (Right) Abundance ratio relative to Fe relative to the solar abundance ratio for nuclei produced in Type Ia SN explosions for the WDD2 delayed-detonation model. The weak rates of GXPF1J are used. Solid (dashed) lines show the results with (without) the SCR effects for the weak rates. Taken from [26]

yields of elements are obtained with the e-capture rates of GXPF1J ($21 \leq Z \leq 32$) and KBF (other Z) for both the W7 and WDD2 explosion models. The over-production problem is now found to be suppressed within a factor of about twice as shown in Fig. 4 for the production yields for the WDD2 model [23,26].

The present work was supported in part by JSPS KAKENHI grant No. JP19K03855.

References

- [1] B. A. Brown, and W. A. Richter, Phys. Rev. C **74**, 034315 (2006).
- [2] H. Toki, T. Suzuki, K. Nomoto, S. Jones, and R. Hirschi, Phys. Rev. C **88**, 015806 (2013).
- [3] T. Suzuki, H. Toki and K. Nomoto, Astrophys. J. **817**, 163 (2016).
- [4] S. Jones, R. Hirschi, K. Nomoto et al., Astrophys. J **772**, 150 (2013).
- [5] N. Itoh, N. Tomizawa, M. Tamamura and S. Wanajo, Astrophys. J. **579**, 380 (2002).
- [6] S. Ichimaru, Rev. Mod. Phys. **65**, 255 (1993).
- [7] T. Oda, M. Hino, K. Muto, M. Takahara and K. Sato, At. Data and Nucl. Data Tables **56**, 231 (1994).
- [8] E. K. Warburton, J. A. Becker and B. A. Brown, Phys. Rev. C **41**, 1147 (1990).
- [9] H. Schatz et al., Nature **505**, 62 (2014).
- [10] W.-J. Ong et al., Phys. Rev. Lett. **125**, 262701 (2020).
- [11] K. Takayanagi, Nucl. Phys. A **852**, 61 (2011); ibid. **864**, 91 (2011).
- [12] T. Otsuka, A. Gade, O. Sorlin, T. Suzuki and Y. Utsuno, Rev. Mod. Phys. **92**, 015002 (2020).
- [13] N. Tsunoda, T. Otsuka, N. Shimizu, M. Hjorth-Jensen, K. Takayanagi and T. Suzuki, Phys. Rev. C **95**, 021304 (2017).
- [14] J. Fujita and H. Miyazawa, Prog. Theor. Phys. **17**, 360 (1957).
- [15] Y. Utsuno, T. Otsuka, T. Mizusaki and M. Honma, Phys. Rev. C **60**, 054315 (1999).
- [16] J. R. Terry et al., Phys. Rev. C **77**, 014316 (2008).
- [17] M. Honma, T. Otsuka, T. Mizusaki, M. Hjorth-Jensen and B. A. Brown, J. Phys. Conf. Ser. **20**, 7 (2005).
- [18] M. Sasano et al., Phys. Rev. Lett. **107**, 202501 (2012).
- [19] T. Suzuki, M. Honma, K. Higashiyama et al., Phys. Rev. C **79**, 061603 (2009).
- [20] E. Caurier, G. Martinez-Pinedo, G. F. Nowacki, A. Poves and A. P. Zuker, Rev. Mod. Phys. **77**, 427 (2005).
- [21] K. Langanke and G. Martinez-Pinedo, At. Data and Nucl. Data Tables **79**, 1 (2001).
- [22] A. L. Cole et al., Phys. Rev. C **86**, 015809 (2012).
- [23] K. Mori, M. A. Famiano, T. Kajinoi, T. Suzuki et al., Astrophys. J. **833**, 179 (2016).

- [24] G. M. Fuller, W. A. Fowler and M. J. Newman, *Astrophys. J.* **252**, 715 (1982); *Astrophys. J. Suppl.* **48**, 279 (1982).
- [25] K. Iwamoto, F. Brachwitz, K. Nomoto et al., *Astrophys. J. Suppl.* **125**, 439 (1999).
- [26] K. Mori, T. Suzuki, M. Honma, M. A. Famiano, T. Kajino, M. Kusakabe and A. B. Balantekin, *Astrophys. J.* **904**, 29 (2020).